bioRxiv preprint doi: https://doi.org/10.1101/2019.12.20.884197; this version posted December 20, 2019. The copyright holder for this preprint (which was not certified by peer review) is the author/funder, who has granted bioRxiv a license to display the preprint in perpetuity. It is made available under aCC-BY 4.0 International license.

Genetic background and diet affect brown adipose gene co-expression – metabolic associations

Caryn Carson[1] and Heather A Lawson[1,#]

[1]Department of Genetics, Washington University School of Medicine, 660 South Euclid Ave, Saint Louis, MO, USA

[#]Corresponding author
660 South Euclid Ave
Campus Box 8232
Saint Louis, MO, 63110
ph: 314-362-7269, fax: 314-362-7855

bioRxiv preprint doi: https://doi.org/10.1101/2019.12.20.884197; this version posted December 20, 2019. The copyright holder for this preprint (which was not certified by peer review) is the author/funder, who has granted bioRxiv a license to display the preprint in perpetuity. It is made available under aCC-BY 4.0 International license.

Abstract

Adipose is a dynamic endocrine organ that is critical for regulating metabolism and is highly responsive to nutritional environment. Brown adipose tissue is an exciting potential therapeutic target, however there are no systematic studies of gene-by-environment interactions affecting function of this organ. We leveraged a weighted gene co-expression network analysis to identify transcriptional networks in brown adipose tissue from LG/J and SM/J inbred mice fed high or low fat diets, and correlate these networks with metabolic phenotypes. We identified 8 primary gene network modules associated with variation in obesity and diabetes-related traits. Four modules were enriched for metabolically relevant processes such as immune and cytokine response, cell division, peroxisome functions, and organic molecule metabolic processes. The relative expression of genes in these modules is highly dependent on both genetic background and dietary environment. Genes in the immune/cytokine response and cell division modules are particularly highly expressed in high fat-fed SM/J mice, which show unique brown adipose-dependent remission of diabetes. The interconnectivity of genes in these modules is also heavily dependent on diet and strain, with most genes showing both higher expression and co-expression under the same context. We highlight 4 candidate genes, *Col28a1*, *Cyp26b1*, *Bmp8b*, and *Kcnj14*, that have distinct expression patterns among strain-by-diet contexts and fall under metabolic QTL previously mapped in an F_{16} generation of an advanced intercross between these two strains. Each of these genes have some connection to obesity and diabetes-related traits, but have not been studied in brown adipose tissue. In summary, our results provide important insights into the relationship between brown adipose and systemic metabolism by being the first gene-by-environment study of brown adipose transcriptional networks and introducing novel candidate genes for follow-up studies of biological mechanisms of action.

bioRxiv preprint doi: https://doi.org/10.1101/2019.12.20.884197; this version posted December 20, 2019. The copyright holder for this preprint (which was not certified by peer review) is the author/funder, who has granted bioRxiv a license to display the preprint in perpetuity. It is made available under aCC-BY 4.0 International license.

Author Summary

Research on brown adipose tissue is a promising new avenue for understanding and potentially treating metabolic dysfunction. However, we do not know how genetic background interacts with dietary environment to affect the brown adipose transcriptional response, and how this might affect systemic metabolism. Here we report the first investigation of gene-by-environment interactions on brown adipose gene expression networks associating with multiple obesity and diabetes-related traits. We identified 8 primary networks correlated with variation in these traits in mice, including networks enriched for immune and cytokine response, cell division, organic molecule metabolism, and peroxisome genes. Characterizing these networks and their distinct diet-by-strain expression and co-expression patterns is an important step towards understanding how brown adipose tissue responds to an obesogenic diet, how this response affects metabolism, and how this can be modified by genetic variation.

Introduction

Obesity and associated metabolic disorders are reaching epidemic prevalence world-wide. While some of this prevalence is the result of increasingly inactive lifestyles and changing dietary norms, the hundreds of genome-wide association study (GWAS) 'hits' for obesity and metabolic diseases indicate there is also a strong genetic component [1,2]. Thus it is critical to understand how gene-by-environment interactions are contributing to metabolic dysfunction. Such interactions have been shown to underlie variation in obesity and diabetes risk [3–8], and many individual genes have been identified with natural variants in human populations affecting metabolic response to environmental perturbations [9–14]. Research in animal models, in particular mouse models, has been used to manipulate dietary intake and environment in order to better understand the gene-by-environment interactions most relevant to human metabolism [15–19]. Frequently, studies of obesity in mice look at adipose tissue as a primary metabolic

bioRxiv preprint doi: https://doi.org/10.1101/2019.12.20.884197; this version posted December 20, 2019. The copyright holder for this preprint (which was not certified by peer review) is the author/funder, who has granted bioRxiv a license to display the preprint in perpetuity. It is made available under aCC-BY 4.0 International license.

78 organ, with relatively recent focus on brown adipose tissue as a pro-health therapeutic target for
79 obesity [20].

80 Brown adipose tissue is distinct from white adipose tissue and has mostly been studied
81 for its role in non-shivering thermogenesis, the release of energy as heat through the activity of
82 UCP1 [21,22]. Brown adipose tissue is found in adult humans [23,24] and increased brown
83 adipose activity is associated with a healthier metabolic profile [25] and lower body fat percentage
84 [26]. It is also associated with amelioration of elevated plasma lipid levels in a hyperlipidemic
85 mouse model [27] and remission of the metabolic dysfunction associated with impaired pancreatic
86 islet function in a mouse model of type I diabetes [28]. Mice lacking brown adipose tissue develop
87 obesity and metabolic dysfunction [29] that is independent from the loss of thermogenic UCP1
88 activity [21,30,31], indicating that brown adipose contributes to healthy metabolism through
89 thermogenesis-independent mechanisms. Several studies have sought to identify potential
90 metabolically-relevant brown adipose cytokines, or “batokines” underlying these mechanisms
91 [32–34]. However, very little research has focused on understanding the potential regulation of
92 these batokines, and most studies regarding transcriptional networks in brown adipose tissue
93 have focused exclusively on identifying regulators and effectors of nonshivering thermogenesis
94 and brown adipocyte identity [35,36,45–49,37–44].

95 We wanted to more broadly understand the transcriptional networks existing within brown
96 adipose tissue, to investigate how these networks are affected by genetic background and dietary
97 environment, and determine how they associate with metabolic variation. To do this, we chose to
98 study SM/J and LG/J inbred mice fed high and low fat diets. These strains both respond to a high
99 fat diet with obesity, elevated fasting glucose, and impaired glucose tolerance at 20 weeks of age
100 [50]. However, by 30 weeks, high fat-fed SM/J mice resolve their glycemic dysfunction [51]. This
101 occurs concurrently with a dramatic expansion of their interscapular brown adipose depots,
102 making SM/J mice a unique and intriguing model system in which to investigate brown adipose
103 transcriptional networks, how they correlate with metabolic traits, and how they are affected by

bioRxiv preprint doi: https://doi.org/10.1101/2019.12.20.884197; this version posted December 20, 2019. The copyright holder for this preprint (which was not certified by peer review) is the author/funder, who has granted bioRxiv a license to display the preprint in perpetuity. It is made available under aCC-BY 4.0 International license.

dietary environment. In this study, we employed a weighted gene co-expression network analysis (WGCNA) [52,53] and identified eight primary gene modules within brown adipose tissue that correlate with one or more obesity and diabetes-related phenotypes. The expression profile of genes within these modules is dependent on both strain and dietary contexts, indicating gene-by-environment interactions contribute significantly to variation in brown adipose tissue function. This study is an important first step in elucidating metabolically-relevant brown adipose transcriptional networks, how they are affected by genetic background and diet, and how they contribute to systemic metabolism through mechanisms beyond thermogenesis.

Results

Brown adipose expression and metabolic traits vary among strain and diet contexts

To understand how brown adipose gene expression in different genetic backgrounds contributes to metabolic variation in different environmental contexts, we raised LG/J and SM/J mice on isocaloric high and low fat diets. The mice were extensively phenotyped (**Supplementary Table 1**) and RNA sequencing of brown adipose was used to assess both mRNA and noncoding RNA transcript levels. To understand how genetic background and diet interact to affect the brown adipose transcriptome, samples were clustered based on gene expression (**Figure 1, top**). Strain is a much better predictor of overall clustering than diet, with the LG/J samples clustering into a single group comprising both diets. The SM/J samples separate into two main clusters, one for each diet, indicating that the SM/J's brown adipose is more responsive to dietary environment. A heatmap is used to visualize the metabolic variation among the strains and diets (**Figure 1, bottom**). Glucose and insulin parameters consistently show higher values in the high fat-fed SM/J's relative to low fat-fed mice or LG/J mice on either diet. Lipid levels are more mixed and variable throughout the entire population. LG/J mice have lower brown adipose to body weight ratios than SM/J mice. Within the SM/J's, high fat-fed mice have both higher body weight and higher brown adipose to body weight ratios than low fat-fed mice.

bioRxiv preprint doi: https://doi.org/10.1101/2019.12.20.884197; this version posted December 20, 2019. The copyright holder for this preprint (which was not certified by peer review) is the author/funder, who has granted bioRxiv a license to display the preprint in perpetuity. It is made available under aCC-BY 4.0 International license.

Modules enriched for immune/cytokine response and cell division correlate with glucose parameters and brown adipose to body weight ratio

To identify gene network modules in brown adipose tissue that associate with the observed variation in metabolic phenotypes, we performed WGCNA [53] on the brown adipose gene expression profiles of all cohorts. An unsigned Topological Overlap Matrix assigned genes to 15 discrete modules and eigenvalues were calculated for each module. We then correlated the module eigenvalues with each metabolic phenotype, and find that 8 of 15 modules show significant correlation with at least one phenotype (**Figure 2**). Four modules show significant correlation with at least three of the 4 glucose and insulin parameters (magenta, blue, brown, and pink) and three modules show significant correlations with both body weight and brown adipose to body weight ratio (midnight blue, turquoise and yellow). The blue and brown modules in particular have significant correlations with both glucose phenotypes and brown adipose to body weight ratio.

To determine if the modules are enriched for particular classes of genes, we employed Gene Ontology (GO) term enrichment within each module (**Supplementary Table 2**). Three modules have multiple enriched GO terms and were assigned a general descriptor term for the top 10 enriched terms: blue = immune/cytokine response, brown = cell division and red = organic molecule metabolic processes. The pink module has only one enriched GO term (peroxisome) while the remaining four modules have no significantly enriched GO terms (at an FDR = 0.05). To focus the remainder of our results, we primarily discuss the four modules with enriched GO terms, however all analyses were performed on the modules without enriched GO terms as well.

Gene expression within network modules varies across both diet and strain contexts

To determine how similar the module-trait relationships are across diets and strains, we analyzed each strain and each diet individually through the WGCNA pipeline (**Supplementary**

bioRxiv preprint doi: https://doi.org/10.1101/2019.12.20.884197; this version posted December 20, 2019. The copyright holder for this preprint (which was not certified by peer review) is the author/funder, who has granted bioRxiv a license to display the preprint in perpetuity. It is made available under aCC-BY 4.0 International license.

Figure 1, Supplementary Table 3). At least one immune or immune/cytokine response module is present in both strains and both diets, however the cell division module only appears in the high fat-fed SM/J brown adipose. This led us to hypothesize that some modules may be driven by expression within a particular cohort. To test this, we performed principal components analysis on the genes within each module (**Figure 3, Supplementary Figure 2**).

Variation in the blue immune/ cytokine response module is driven mainly by strain, which then further separates by diet within strain. It is well-established that white adipose tissue is an immunologically active organ that, in obesity, displays both active and adaptive immune responses that affect systemic metabolism [54,55]. However the immunological role of brown adipose tissue is relatively understudied [56]. Our data indicate that genetic background strongly modifies brown adipose tissue's immunological and cellular signaling processes in response to nutritional environment.

The brown cell division module shows remarkable clustering of the high fat-fed SM/J cohort, which is consistent with our result that enrichment of this term is driven by high fat-fed SM/J mice. Further, high fat-fed SM/J mice have the highest brown adipose to body weight ratios and our previous work showed that the brown adipose expansion observed in these mice is the result of hyperplasia [51]. Both pink peroxisome and red organic molecule processes show moderate diet-by-strain clustering.

Strain-specific variation drives differential expression and differential connectivity within brown adipose gene modules

To identify the genes that are most differentially expressed between the diets and strains we calculated both differential expression and connectivity. Genes passing an FDR threshold of 0.05 are considered differentially expressed, regardless of fold change. Connectivity was calculated as the degree of co-expression of each gene with all other genes. Genes with differences in connectivity having an absolute value above 0.5 between diets and strains are

bioRxiv preprint doi: https://doi.org/10.1101/2019.12.20.884197; this version posted December 20, 2019. The copyright holder for this preprint (which was not certified by peer review) is the author/funder, who has granted bioRxiv a license to display the preprint in perpetuity. It is made available under aCC-BY 4.0 International license.

considered differentially connected. Combining differential expression and differential connectivity between the strains and diets allows us to investigate individual genes in transcriptional networks that are particularly susceptible to differences in diets or genetic backgrounds. To our knowledge this has never been explored in brown adipose tissue.

Genes in the blue immune/ cytokine response, brown cell division, and pink peroxisome modules have increased connectivity in high fat-fed mice regardless of genetic background (**Figure 4A**). This indicates that genes in these modules are more tightly co-expressed under nutritional excess. In contrast, the red organic molecule metabolic processes module has a more even distribution of connectivity, with a trend towards higher connectivity in low fat-fed mice. The distribution of differential expression in each module also shows even numbers of genes upregulated in high or low fat-fed mice (**Figure 4A, Supplementary Figure 3A**). However, genes with the highest differential expression tend to also have differential connectivity, with the majority showing increased expression and increased connectivity in animals fed the same diet.

Analyzing differential expression and connectivity by strain reveals much stronger connectivity in the SM/J strain compared to the LG/J strain in all four of our primary modules (**Figure 4B**) and in two of our four secondary modules (**Supplementary Figure 3B**). Similar to the connectivity-by-diet analysis, genes with high differential expression also have increased connectivity in the same genetic background. However, this may be skewed by the overall quantity of genes that are differentially expressed by strain (n = 4847). To break down connectivity and expression patterns between diets and between strains, we classified genes that showed both differential connectivity and significant differential expression between diets or between strains as potential hub genes. In total, this resulted in 2564 potential hub genes: 659 that are differentially expressed and connected by diet, 2320 by strain, and 415 for diet-by-strain (**Supplementary Table 4**).

To further refine these lists and identify candidates that are likely to be contributing to metabolic variation, we filtered for genes that are differentially connected and differentially

bioRxiv preprint doi: https://doi.org/10.1101/2019.12.20.884197; this version posted December 20, 2019. The copyright holder for this preprint (which was not certified by peer review) is the author/funder, who has granted bioRxiv a license to display the preprint in perpetuity. It is made available under aCC-BY 4.0 International license.

208 expressed with a fold change ≥ 2. This produced a list of 25 genes, 13 of which belong to the
209 blue immune/ cytokine or brown cell division modules (**Supplementary Table 5**). Interestingly,
210 these 13 genes are all upregulated and have higher connectivity in the high fat-fed SM/J cohort,
211 indicating that the brown adipose of SM/J mice is particularly responsive to nutritional excess.
212 This is consistent with our previous work showing brown adipose tissue-dependent
213 resolution of diabetes in high fat-fed SM/J mice [51]. Twenty-four of these hub genes contain
214 small nucleotide variants between the LG/J and SM/J strains [57] (**Supplementary Table 6**),
215 which could be contributing to the gene-by-environmental differential expression patterns we
216 observe. Further, four of these genes, *Col28a1*, *Bmp8b*, *Cyp26b1*, and *Kcnj14*, fall within the
217 support intervals of metabolic quantitative trait loci (QTL) mapped in an F_{16} advanced intercross
218 of the SM/J and LG/J strains (**Table 1; Supplementary Figure 4**) [58,59]. These genes represent
219 actionable candidates that can be tested for their function in brown adipose tissue and effects on
220 obesity and systemic metabolism.
221
222 **Discussion**
223 Adipose is a dynamic endocrine organ that is critical for regulating systemic metabolism.
224 Further, adipose tissue function displays a high degree of plasticity under different nutritional
225 conditions [60–62]. Though brown adipose has high therapeutic potential for obesity and related
226 metabolic disorders, research on this tissue is in its infancy and most genetic studies focus on
227 identifying the factors involved in its thermogenic function and in determining brown adipocyte
228 identity. Yet recent research reveals that brown adipose is a source of endocrine signals with both
229 anti-diabetic and anti-obesogenic properties [63,64]. High fat diet has been shown to alter brown
230 adipose activity and blunt its positive effects on systemic metabolism [65,66]. Yet, as illustrated
231 by numerous studies, dietary response is heavily dependent on genetic background [16,17,73–
232 75,50,51,67–72]. Here we present the first study on the effects of genetic background and diet on
233 brown adipose transcriptional networks associating with metabolic variation.

bioRxiv preprint doi: https://doi.org/10.1101/2019.12.20.884197; this version posted December 20, 2019. The copyright holder for this preprint (which was not certified by peer review) is the author/funder, who has granted bioRxiv a license to display the preprint in perpetuity. It is made available under aCC-BY 4.0 International license.

We illustrate that the SM/J brown adipose transcriptome is more susceptible to dietary perturbations in comparison with the LG/J strain (**Figure 1**). The LG/J and SM/J strains are frequently used in metabolic studies because they vary in their metabolic response to dietary fat [50,58,59,76,77]. We recently demonstrated that high fat-fed SM/J mice dramatically expand their interscapular brown adipose depots and that contemporary with this expansion, mice enter diabetic remission [51]. Understanding the genetic underpinnings of this phenomenon could open new avenues for understanding novel biology and highlight therapeutic targets for obesity-related metabolic dysfunction.

We identified eight primary gene co-expression modules that are highly correlated with obesity and diabetes traits (**Figure 2**). Four of these modules show significant over-representation of genes belonging to biological categories that affect adipose function and systemic metabolism: immune/cytokine response, peroxisomes, organic metabolic processes, and cell division. Genes involved in immune and cytokine response show a conserved network correlating with glucose and insulin traits (**Figure 3, Supplementary Figure 1**). This is consistent with previous work relating hyperglycemia, hyperinsulinemia, and other diabetes-related traits with inflammatory markers and immune infiltration of adipose [55,78–80]. Peroxisome genes are essential to lipid metabolism, and have been shown to regulate the thermogenic function of both brown and beige adipocytes [81]. Genes composing the organic metabolic processes category include those that perform essential functions in glucose and lipid uptake (**Supplementary Table 3**). Genes involved in cell division form a network specific to high fat-fed SM/J mice, and strongly correlate with glucose and insulin traits as well as with brown adipose to body weight ratio (**Figure 3, Supplementary Figure 1**). The gene-by-environmental specificity of this module, its association with glycemic parameters, and the unique characteristics of brown adipose in the SM/J strain [82], indicate that the genes in this module are compelling candidates for further studies of biological mechanisms of action of brown adipose and systemic metabolism.

bioRxiv preprint doi: https://doi.org/10.1101/2019.12.20.884197; this version posted December 20, 2019. The copyright holder for this preprint (which was not certified by peer review) is the author/funder, who has granted bioRxiv a license to display the preprint in perpetuity. It is made available under aCC-BY 4.0 International license.

We highlight 4 genes that fall in QTL previously mapped in an F_{16} generation of a LG/J x SM/J advanced intercross population (**Table 1**) [58,83]. *Kcnj14*, potassium inwardly rectifying channel subfamily J member 14, is part of the blue immune/cytokine response module. It is an essential membrane protein and inward-rectifier potassium channel that may play a role in glucose uptake in target tissues of insulin. Although *Kcnj14* is understudied, in vivo glucose uptake experiments in mice suggest that disruption of potassium channels affect insulin-stimulated glucose uptake in white adipose [84]. Other studies have shown that potassium channel knock-out mice have hyperlipidemic brown adipose tissue [85]. *Cyp26b1*, cytochrome P450 family 26 subfamily B member 1, is also part of the blue immune/cytokine response module. It is a retinoic acid hydroxylase that regulates cellular concentrations of all-trans-retinoic acid. Retinoic acid is a vitamin A derivative that is essential for cell growth and differentiation. Early studies show that retinoids, including retinoic acid, play an essential role in adipose differentiation [86,87], and a recent study found that retinoic acid mediates adipogenic defects in human white adipose-derived stem cells [88]. *Col28a1*, collagen type XXVIII alpha 1, is part of the brown cell division module. It belongs to a class of collagens involved in extracellular matrix (ECM). The ECM is a critical component in cellular signaling, either through direct interaction with cell-surface receptors or through the ability to regulate growth factor bioavailability [89]. Collagen is highly enriched in adipocytes, and its depletion is associated with metabolic dysfunction [90]. *Bmp8b*, bone morphogenic protein 8b, is part of the red organic metabolic processes module. Of these four candidates, only *Bmp8b* has been studied in brown adipose. It is secreted by brown adipocytes and amplifies the thermogenic response of cells by increasing sensitivity to adrenergic input [91,92].

Gene-by-environment interactions are critical for understanding the intricacies and nuances of obesity and metabolic dysfunction, and for identifying potential therapeutic targets. Though there is increasing interest in brown adipose tissue as a potential therapeutic target for such diseases, there have been no studies on gene-by-environment interactions in brown adipose

bioRxiv preprint doi: https://doi.org/10.1101/2019.12.20.884197; this version posted December 20, 2019. The copyright holder for this preprint (which was not certified by peer review) is the author/funder, who has granted bioRxiv a license to display the preprint in perpetuity. It is made available under aCC-BY 4.0 International license.

285 tissue, and few studies on brown adipose in mouse strains other than C57BL/6J. Our results
286 indicate that gene-by-environment interactions significantly contribute to variation in brown
287 adipose transcriptional networks. Understanding how genetic variation mediates brown adipose
288 tissue's response to an obesogenic diet will be key to harnessing its therapeutic potential. Further,
289 the unique transcriptomic profile of high fat-fed SM/J brown adipose tissue and its correlation with
290 diabetic remission [51] highlight compelling candidates for understanding brown adipose tissue's
291 endocrine function and biological mechanisms of action beyond thermogenesis.
292
293 **Materials and Methods**
294 *Sample Collection and Sequencing*
295 Experimental animals were generated from SM/J (RRID:IMSR_JAX:000687) and LG/J
296 (RRID:IMSR_JAX:000675) mice obtained from The Jackson Laboratory (Bar Harbor, ME) at the
297 Washington University School of Medicine. All experiments were approved by the Institutional
298 Animal Care and Use Committee in accordance with the National Institutes of Health guidelines
299 for the care and use of laboratory animals. Mice were randomly weaned onto a high fat diet (42%
300 kcal from fat; Teklad TD88137) or an isocaloric low fat diet (15% kcal from fat; Research Diets
301 D12284) and fed *ad libitum*. Additional mouse maintenance details and phenotype collection are
302 described extensively in Carson et al., 2019 [51], and summary statistics for each cohort are
303 provided in **Supplementary Table 1**.
304 Total RNA was isolated from intrascapular brown adipose tissue using the RNeasy Lipid
305 Tissue Kit (QIAgen). RiboZero (Illumina) libraries were sequenced at 2x100 paired end reads on
306 an Illumina HiSeq 4000. Reads were aligned against LG/J and SM/J custom genomes using
307 STAR [57,93]. Read counts were normalized via upper quartile normalization and a minimum
308 normalized read depth of 10 was required. Additional sequencing and alignment details are
309 provided in Carson et al., 2019 [51].
310

bioRxiv preprint doi: https://doi.org/10.1101/2019.12.20.884197; this version posted December 20, 2019. The copyright holder for this preprint (which was not certified by peer review) is the author/funder, who has granted bioRxiv a license to display the preprint in perpetuity. It is made available under aCC-BY 4.0 International license.

311 *Gene co-expression and phenotype associations*

312 The Weighted Gene Co-Expression Network Analysis (WGCNA) R package was used to
313 determine gene co-expression modules and their correlation with metabolic traits [53]. Briefly,
314 edgeR-normalized counts for each gene were converted to a standard normal. Genes with
315 standard deviation of at least 0.25 were deemed biologically variable and used in the subsequent
316 analysis (7740 genes total) [94]. Samples were clustered based on expression of all genes and
317 two low fat LG/J samples were removed as outliers before continuing with the analysis. The
318 adjacency matrix was created from Pearson's correlations calculated between all genes and
319 raised to a power β of 12, chosen based on a scale-free topology index above 0.9. Raising the
320 absolute value of the correlation by this power is done to emphasize high correlations at the
321 expense of low correlations [95].

322 The blockwiseModules function was used to create an unsigned Topological Overlap
323 Measure using the adjacency matrix and to identify modules of highly interconnected genes. Each
324 module was assigned a color for identification. Module eigengenes were calculated as the first
325 principal component for each module, and Pearson's correlations were calculated between each
326 module eigengene and each phenotype to estimate module-trait relationships. Module-trait
327 correlations were considered significant at an FDR-corrected p-value < 0.05 and an absolute
328 correlation of at least 0.5. Gene Ontology term enrichment was calculated for individual modules
329 from a background of all expressed genes in the dataset. Modules were considered enriched for
330 a term at a Bonferoni-corrected p-value less < 0.05. Modules with no significantly enriched terms
331 were designated as "No Enrichment" and modules with multiple enriched terms were classified
332 with an overarching description of the top ten significantly enriched terms.

333

334 *Differential Connectivity*

335 Differential connectivity is a measure of the differences in gene interactions between high
336 and low fat-fed mice or between SM/J and LG/J mice. Four subnetworks were created (HF, LF,

bioRxiv preprint doi: https://doi.org/10.1101/2019.12.20.884197; this version posted December 20, 2019. The copyright holder for this preprint (which was not certified by peer review) is the author/funder, who has granted bioRxiv a license to display the preprint in perpetuity. It is made available under aCC-BY 4.0 International license.

LG/J, SM/J) with the same 7740 genes as in the full network analysis. Within each subnetwork, we assigned genes to modules and defined module-trait relationships. The connectivity of each gene was calculated in each network with an adjacency matrix as a measure of how correlated the gene is with all other genes in the network. Differential connectivity was calculated between diets or strains for each gene $kDiff = \frac{HF - LF}{HF + LF}$ or $kDiff = \frac{SM - LG}{SM + LG}$ to provide values between -1 and 1. Genes were considered differentially connected when one cohort had three times the connectivity of the other cohort, or an absolute kDiff > 0.5. Genes with positive differential connectivity are more highly connected in the HF or SM cohorts than in the LF or LG cohorts. To further narrow down genes into those most likely to be biologically impactful hub genes, differential expression between diets and strains was calculated for all genes using the exactTest function in edgeR. Genes with an FDR-corrected p-value < 0.05 are considered to be significantly differentially expressed. Hub genes in diet or strain contexts were called as those with both an absolute differential connectivity value > 0.5 and significant differential expression in the same comparison.

Acknowledgements

This work was supported by the Washington University Department of Genetics, the Diabetes Research Center at Washington University (P30DK020579), the NIH NIDDK (K01 DK095003) to HAL and NIH NIGM (T32 GM007067) to CC.

References

1. Fall T, Ingelsson E. Genome-wide association studies of obesity and metabolic syndrome. Mol Cell Endocrinol. 2014;382: 740–757. doi:10.1016/j.mce.2012.08.018

2. Cheng M, Mei B, Zhou Q, Zhang M, Huang H, Han L, et al. Computational analyses of

bioRxiv preprint doi: https://doi.org/10.1101/2019.12.20.884197; this version posted December 20, 2019. The copyright holder for this preprint (which was not certified by peer review) is the author/funder, who has granted bioRxiv a license to display the preprint in perpetuity. It is made available under aCC-BY 4.0 International license.

obesity associated loci generated by genome-wide association studies. PLoS One. 2018;13: 1–13. doi:10.1371/journal.pone.0199987

3. Nagpal S, Gibson G, Marigorta UM. Pervasive modulation of obesity risk by the environment and genomic background. Genes (Basel). 2018;9. doi:10.3390/genes9080411

4. Abadi A, Alyass A, Robiou du Pont S, Bolker B, Singh P, Mohan V, et al. Penetrance of Polygenic Obesity Susceptibility Loci across the Body Mass Index Distribution. Am J Hum Genet. 2017;101: 925–938. doi:10.1016/j.ajhg.2017.10.007

5. Li X, Qi L. Gene – Environment Interactions on Body Fat Distribution. Int J Mol Sci. 2019;20. doi:10.3390/ijms20153690

6. Franks PW. Gene × environment interactions in type 2 diabetes. Curr Diab Rep. 2011;11: 552–561. doi:10.1007/s11892-011-0224-9

7. Llewellyn C, Wardle J. Behavioral susceptibility to obesity: Gene-environment interplay in the development of weight. Physiol Behav. 2015;152: 494–501. doi:10.1016/j.physbeh.2015.07.006

8. Schrempft S, Van Jaarsveld CHM, Fisher A, Herle M, Smith AD, Fildes A, et al. Variation in the Heritability of Child Body Mass Index by Obesogenic Home Environment. JAMA Pediatr. 2018;172: 1153–1160. doi:10.1001/jamapediatrics.2018.1508

9. Benson KK, Hu W, Weller AH, Bennett AH, Chen ER, Khetarpal SA, et al. Natural human genetic variation determines basal and inducible expression of PM20D1 , an obesity-associated gene. PNAS. 2019; 1–11. doi:10.1073/pnas.1913199116

10. Wang H, Zhang F, Zeng J, Wu Y, Kemper KE, Xue A, et al. Genotype-by-environment interactions inferred from genetic effects on phenotypic variability in the UK Biobank. Sci Adv. 2019;5: eaaw3538. doi:10.1126/sciadv.aaw3538

11. Snyder EE, Walts B, Perusse L, Chagnon YC, Weisnagel SJ, Rankinen T, et al. The human obesity gene map: The 2003 update. Obes Res. 2004;12: 369–439.

bioRxiv preprint doi: https://doi.org/10.1101/2019.12.20.884197; this version posted December 20, 2019. The copyright holder for this preprint (which was not certified by peer review) is the author/funder, who has granted bioRxiv a license to display the preprint in perpetuity. It is made available under aCC-BY 4.0 International license.

12. Stutzmann F, Tan K, Vatin V, Dina C, Jouret B, Tichet J, et al. Prevalence of melanocortin-4 receptor deficiency in europeans and their age-dependent penetrance in multigenerational pedigrees. Diabetes. 2008;57: 2511–2518. doi:10.2337/db08-0153

13. Pigeyre M, Yazdi FT, Kaur Y, Meyre D. Recent progress in genetics, epigenetics and metagenomics unveils the pathophysiology of human obesity. Clin Sci. 2016;130: 943–986. doi:10.1042/CS20160136

14. Williams Amy AL, Jacobs Suzanne SBR, Moreno-Macías H, Huerta-Chagoya A, Churchhouse C, Márquez-Luna C, et al. Sequence variants in SLC16A11 are a common risk factor for type 2 diabetes in Mexico. Nature. 2014;506: 97–101. doi:10.1038/nature12828

15. Brockmann GA, Bevova MR. Using mouse models to dissect the genetics of obesity. Trends Genet. 2002;18: 367–376. doi:10.1016/S0168-9525(02)02703-8

16. Eberhart GP, West DB, Boozer CN, Atkinson RL. Insulin sensitivity of adipocytes from inbred mouse strains resistant or sensitive to diet-induced obesity. Am J Physiol - Regul Integr Comp Physiol. 1994;266. doi:10.1152/ajpregu.1994.266.5.r1423

17. West DB, Waguespack J, McCollister S. Dietary obesity in the mouse: Interaction of strain with diet composition. Am J Physiol - Regul Integr Comp Physiol. 1995;268. doi:10.1152/ajpregu.1995.268.3.r658

18. Lawson H, Cheverud J. Metabolic Syndrome Components in Murine Models. Endocrine, Metab Immune Disord - Drug Targets. 2010;10: 25–40. doi:10.2174/187153010790827948

19. Wayhart JP, Lawson HA. Animal Models of Metabolic Syndrome. Second Edi. Animal Models for the Study of Human Disease: Second Edition. Elsevier Inc.; 2017. doi:10.1016/B978-0-12-809468-6.00009-7

20. Cannon B, Nedergaard J. Brown adipose tissue: function and physiological significance. Physiol Rev. 2004;84: 277–359. doi:10.1152/physrev.00015.2003

21. Feldmann HM, Golozoubova V, Cannon B, Nedergaard J. UCP1 Ablation Induces Obesity

bioRxiv preprint doi: https://doi.org/10.1101/2019.12.20.884197; this version posted December 20, 2019. The copyright holder for this preprint (which was not certified by peer review) is the author/funder, who has granted bioRxiv a license to display the preprint in perpetuity. It is made available under aCC-BY 4.0 International license.

and Abolishes Diet-Induced Thermogenesis in Mice Exempt from Thermal Stress by Living at Thermoneutrality. Cell Metab. 2009;9: 203–209. doi:10.1016/j.cmet.2008.12.014

22. Rothwell NJ, Stock MJ. A role for brown adipose tissue in diet-induced thermogenesis. Nature. 1979;281: 31–35.

23. Cypess AM, Lehman S, Williams G, Tal I, Rodman D, Goldfine AB, et al. Identification and importance of brown adipose tissue in adult humans. N Engl J Med. 2009;360: 1509–17. doi:10.1056/NEJMoa0810780

24. Virtanen KA, Lidell ME, Orava J, Heglind M, Westergren R, Niemi T, et al. Functional Brown Adipose Tissue in Healthy Adults. N Engl J Med. 2009;360: 1518–1525. doi:10.1056/NEJMoa0808949

25. Chechi K, Carpentier AC, Richard D. Understanding the brown adipocyte as a contributor to energy homeostasis. Trends Endocrinol Metab. 2013;24: 408–420. doi:10.1016/j.tem.2013.04.002

26. van Marken Lichtenbelt WD, Vanhommerig JW, Smulders NM, Drossaerts JM, Kemerink GJ, Bouvy ND, et al. Cold-activated brown adipose tissue in healthy men. NEnglJ Med. 2009;360: 1500–1508.

27. Bartelt A, Bruns OT, Reimer R, Hohenberg H, Ittrich H, Peldschus K, et al. Brown adipose tissue activity controls triglyceride clearance. Nat Med. 2010;17: 200–205. doi:10.1038/nm.2297

28. Gunawardana SC, Piston DW. Reversal of type 1 diabetes in mice by brown adipose tissue transplant. Diabetes. 2012;61: 674–682. doi:10.2337/db11-0510

29. Hamann A, Flier JS, Lowell BB. Decreased Brown Fat Markedly Enhances Susceptibility to Diet-Induced Obesity, Diabetes, and Hyperlipidemia. Endocrinology. 1996;137: 21–29.

30. Enerbäck S, Jacobsson a, Simpson EM, Guerra C, Yamashita H, Harper ME, et al. Mice lacking mitochondrial uncoupling protein are cold-sensitive but not obese. Nature. 1997. pp. 90–94. doi:10.1038/387090a0

bioRxiv preprint doi: https://doi.org/10.1101/2019.12.20.884197; this version posted December 20, 2019. The copyright holder for this preprint (which was not certified by peer review) is the author/funder, who has granted bioRxiv a license to display the preprint in perpetuity. It is made available under aCC-BY 4.0 International license.

440 31. Liu X, Rossmeisl M, Mcclaine J, Kozak LP. Paradoxical resistance to diet-induced obesity
441 in UCP1-deficient mice. J Clin Invest. 2003;111: 399–407.
442 doi:10.1172/JCI200315737.Introduction
443 32. Wang GX, Zhao XY, Lin JD. The brown fat secretome: Metabolic functions beyond
444 thermogenesis. Trends Endocrinol Metab. 2015;26: 231–237.
445 doi:10.1016/j.tem.2015.03.002
446 33. Villarroya J, Cereijo R, Giralt M, Villarroya F. Secretory Proteome of Brown Adipocytes in
447 Response to cAMP-Mediated Thermogenic Activation. Front Physiol. 2019;10: 1–8.
448 doi:10.3389/fphys.2019.00067
449 34. Deshmukh AS, Peijs L, Nielsen S, Bayarri-Olmos R, Larsen TJ, Jespersen NZ, et al.
450 Proteomics-based comparative mapping of the human brown and white adipocyte
451 secretome reveals EPDR1 as a novel batokine. bioRxiv. 2018; 402867.
452 doi:10.1101/402867
453 35. Emmett MJ, Lim H-W, Jager J, Richter HJ, Adlanmerini M, Peed LC, et al. Histone
454 Deacetylase 3 Prepares Brown Adipose Tissue for Acute Thermogenic Challenge. Nature.
455 2018;546: 544–548. doi:10.1038/nature22819
456 36. Harms M, Seale P. Brown and beige fat: development, function and therapeutic potential.
457 Nat Med. 2013;19: 1252–1263. doi:10.1038/nm.3361
458 37. He L, Tang M, Xiao T, Liu H, Liu W, Li G, et al. Obesity-associated miR-199a/214 cluster
459 inhibits adipose browning via PRDM16-PGC-1α transcriptional network. Diabetes.
460 2018;67: 2585–2600. doi:10.2337/db18-0626
461 38. Mori MA, Thomou T, Boucher J, Lee KY, Lallukka S, Kim JK, et al. Altered miRNA
462 processing disrupts brown/white adipocyte determination and associates with
463 lipodystrophy. J Clin Invest. 2014;124: 3339–3351. doi:10.1172/JCI73468
464 39. Loft A, Forss I, Mandrup S. Genome-Wide Insights into the Development and Function of
465 Thermogenic Adipocytes. Trends Endocrinol Metab. 2017;28: 104–120.

bioRxiv preprint doi: https://doi.org/10.1101/2019.12.20.884197; this version posted December 20, 2019. The copyright holder for this preprint (which was not certified by peer review) is the author/funder, who has granted bioRxiv a license to display the preprint in perpetuity. It is made available under aCC-BY 4.0 International license.

doi:10.1016/j.tem.2016.11.005

40. Sun L, Xie H, Mori MA, Alexander R, Yuan B, Hattangadi SM, et al. Mir193b-365 is essential for brown fat differentiation. Nat Cell Biol. 2011;13: 958–965. doi:10.1038/ncb2286

41. Trajkovski M, Ahmed K, Esau CC, Stoffel M. MyomiR-133 regulates brown fat differentiation through Prdm16. Nat Cell Biol. 2012;14: 1330–1335. doi:10.1038/ncb2612

42. Mori M, Nakagami H, Rodriguez-Araujo G, Nimura K, Kaneda Y. Essential role for miR-196a in brown adipogenesis of white fat progenitor cells. PLoS Biol. 2012;10. doi:10.1371/journal.pbio.1001314

43. Seale P, Conroe HM, Estall J, Kajimura S, Frontini A, Ishibashi J, et al. Prdm16 determines the thermogenic program of subcutaneous white adipose tissue in mice. J Clin Invest. 2011;121: 96–105. doi:10.1172/JCI44271

44. Cui X, You L, Li Y, Zhu L, Zhang F, Xie K, et al. A transcribed ultraconserved noncoding RNA, uc.417, serves as a negative regulator of brown adipose tissue thermogenesis. FASEB J. 2016;30: 4301–4312. doi:10.1096/fj.201600694R

45. Cheng Y, Jiang L, Keipert S, Zhang S, Hauser A, Graf E, et al. Prediction of Adipose Browning Capacity by Systematic Integration of Transcriptional Profiles. Cell Rep. 2018;23: 3112–3125. doi:10.1016/j.celrep.2018.05.021

46. García MC, Tovar S, Pazos P, Diéguez C, Lima L, González-Touceda D. Divergent responses to thermogenic stimuli in BAT and subcutaneous adipose tissue from interleukin 18 and interleukin 18 receptor 1-deficient mice. Sci Rep. 2015;5: 1–14. doi:10.1038/srep17977

47. Siersbæk MS, Loft A, Aagaard MM, Nielsen R, Schmidt SF, Petrovic N, et al. Genome-Wide Profiling of Peroxisome Proliferator-Activated Receptor Gamma in Primary Epididymal , Inguinal , and Brown Adipocytes Reveals Depot-Selective Binding Correlated with Gene Expression. Mol Cell Biol. 2012;32: 3452–3463. doi:10.1128/MCB.00526-12

bioRxiv preprint doi: https://doi.org/10.1101/2019.12.20.884197; this version posted December 20, 2019. The copyright holder for this preprint (which was not certified by peer review) is the author/funder, who has granted bioRxiv a license to display the preprint in perpetuity. It is made available under aCC-BY 4.0 International license.

48. Yao L, Heuser-Baker J, Herlea-Pana O, Zhang N, Szweda LI, Griffin TM, et al. Deficiency in adipocyte chemokine receptor CXCR4 exacerbates obesity and compromises thermoregulatory responses of brown adipose tissue in a mouse model of diet-induced obesity. FASEB J. 2014;28: 4534–4550. doi:10.1096/fj.14-249797

49. Rajan A, Shi H, Xue B. Class I and II Histone Deacetylase Inhibitors Differentially Regulate Thermogenic Gene Expression in Brown Adipocytes. Sci Rep. 2018;8: 1–11. doi:10.1038/s41598-018-31560-w

50. Ehrich TH, Kenney JP, Vaughn TT, Pletscher LS, Cheverud JM, Thomas H, et al. Diet, Obesity, and Hyperglycemia in LG/J and SM/J Mice. Obes Res. 2003;11: 1400–1410.

51. Carson C, Macias-Velasco JF, Gunawardana S, Miranda MA, Oyama S, Schmidt H, et al. Brown adipose expansion and remission of glycemic dysfunction in obese SM/J mice. bioRxiv. 2019; 724369. doi:10.1101/724369

52. Zhang B, Horvath S. A general framework for weighted gene co-expression network analysis. Stat Appl Genet Mol Biol. 2005;4. doi:10.2202/1544-6115.1128

53. Langfelder P, Horvath S. WGCNA: An R package for weighted correlation network analysis. BMC Bioinformatics. 2008;9. doi:10.1186/1471-2105-9-559

54. Grant RW, Dixit VD. Adipose tissue as an immunological organ. Obesity. 2015;23: 512–518. doi:10.1002/oby.21003

55. Zeyda M, Wernly B, Demyanets S, Kaun C, Hämmerle M, Hantusch B, et al. Severe obesity increases adipose tissue expression of interleukin-33 and its receptor ST2, both predominantly detectable in endothelial cells of human adipose tissue. Int J Obes. 2013;37: 658–665. doi:10.1038/ijo.2012.118

56. Villarroya F, Cereijo R, Gavaldà-Navarro A, Villarroya J, Giralt M. Inflammation of brown/beige adipose tissues in obesity and metabolic disease. J Intern Med. 2018; 0–3. doi:10.1111/joim.12803

57. Nikolskiy I, Conrad DF, Chun S, Fay JC, Cheverud JM, Lawson HA. Using whole-genome

bioRxiv preprint doi: https://doi.org/10.1101/2019.12.20.884197; this version posted December 20, 2019. The copyright holder for this preprint (which was not certified by peer review) is the author/funder, who has granted bioRxiv a license to display the preprint in perpetuity. It is made available under aCC-BY 4.0 International license.

sequences of the LG / J and SM / J inbred mouse strains to prioritize quantitative trait genes and nucleotides. BMC Genomics. 2015;16: 1–12. doi:10.1186/s12864-015-1592-3

58. Lawson HA, Zelle KM, Fawcett GL, Wang B, Pletscher LS, Maxwell TJ, et al. Genetic , epigenetic , and gene-by-diet interaction effects underlie variation in serum lipids in a LG / J × SM / J murine model. J Lipid Res. 2010;51: 2976–2984. doi:10.1194/jlr.M006957

59. Lawson HA, Lee A, Fawcett GL, Wang B, Pletscher LS, Maxwell TJ, et al. The importance of context to the genetic architecture of diabetes-related traits is revealed in a genome-wide scan of a LG / J 3 SM / J murine model. Mamm Genome. 2011;22: 197–208. doi:10.1007/s00335-010-9313-3

60. Sethi JK, Vidal-Puig AJ. Adipose tissue function and plasticity orchestrate nutritional adaptation. J Lipid Res. 2007;48: 1253–1262. doi:10.1194/jlr.R700005-JLR200

61. Haugen F, Drevon CA. The interplay between nutrients and the adipose tissue: Plenary lecture. Proc Nutr Soc. 2007;66: 171–182. doi:10.1017/S0029665107005423

62. Rosen ED, Spiegelman BM. What we talk about when we talk about fat. Cell. 2014;156: 20–44. doi:10.1016/j.cell.2013.12.012

63. Stanford KI, Middelbeek RJ, Townsend KL, An D, Nygaard EB, Hitchcox KM, et al. Brown adipose tissue regulates glucose homeostasis and insulin sensitivity. J Clin Invest. 2013;123: 215–223. doi:10.1172/JCI62308DS1

64. Lowell BB, S-Susulic V, Hamann A, Lawitts JA, Himms-Hagen J, Boyer BB, et al. Development of obesity in transgenic mice after genetic ablation of brown adipose tissue. Nature. 1993;366: 740–742.

65. Shankar K, Kumar D, Gupta S, Varshney S, Rajan S, Srivastava A, et al. Role of brown adipose tissue in modulating adipose tissue inflammation and insulin resistance in high-fat diet fed mice. Eur J Pharmacol. 2019;854: 354–364. doi:10.1016/j.ejphar.2019.02.044

66. Ohtomo T, Ino K, Miyashita R, Chigira M, Nakamura M, Someya K, et al. Chronic high-fat feeding impairs adaptive induction of mitochondrial fatty acid combustion-associated

bioRxiv preprint doi: https://doi.org/10.1101/2019.12.20.884197; this version posted December 20, 2019. The copyright holder for this preprint (which was not certified by peer review) is the author/funder, who has granted bioRxiv a license to display the preprint in perpetuity. It is made available under aCC-BY 4.0 International license.

544 proteins in brown adipose tissue of mice. Biochem Biophys Reports. 2017;10: 32–38.
545 doi:10.1016/j.bbrep.2017.02.002
546 67. Walkley SU, Hunt CE, Clements RS, Lindsey JR. Description of obesity in the PBB/Ld
547 mouse. J Lipid Res. 1978;19: 335–341.
548 68. Surwit RS, Wang S, Petro AE, Sanchis D, Raimbault S, Ricquier D, et al. Diet-induced
549 changes in uncoupling proteins in obesity-prone and obesity-resistant strains of mice. Proc
550 Natl Acad Sci U S A. 1998;95: 4061–4065. doi:10.1073/pnas.95.7.4061
551 69. West DB, Boozer CN, Moody DL, Atkinson RL. Dietary obesity in nine inbred mouse
552 strains. Am J Physiol - Regul Integr Comp Physiol. 1992;262.
553 doi:10.1152/ajpregu.1992.262.6.r1025
554 70. Smith BK, Andrews PK, West DB. Macronutrient diet selection in thirteen mouse strains.
555 Am J Physiol - Regul Integr Comp Physiol. 2000;278: 797–805.
556 doi:10.1152/ajpregu.2000.278.4.r797
557 71. Alexander J, Chang GQ, Dourmashkin JT, Leibowitz SF. Distinct phenotypes of obesity-
558 prone AKR/J, DBA2J and C57BL/6J mice compared to control strains. Int J Obes. 2006;30:
559 50–59. doi:10.1038/sj.ijo.0803110
560 72. Montgomery MK, Hallahan NL, Brown SH, Liu M, Mitchell TW, Cooney GJ, et al. Mouse
561 strain-dependent variation in obesity and glucose homeostasis in response to high-fat
562 feeding. Diabetologia. 2013;56: 1129–1139. doi:10.1007/s00125-013-2846-8
563 73. Chu DT, Malinowska E, Jura M, Kozak LP. C57BL/6J mice as a polygenic developmental
564 model of diet-induced obesity. Physiol Rep. 2017;5: 1–20. doi:10.14814/phy2.13093
565 74. Sims EK, Hatanaka M, Morris DL, Tersey SA, Kono T, Chaudry ZZ, et al. Divergent
566 compensatory responses to high-fat diet between C57Bl6/J and c57BlKS/J inbred mouse
567 strains. Am J Physiol - Endocrinol Metab. 2013;305: 1495–1511.
568 doi:10.1152/ajpendo.00366.2013
569 75. Andrikopoulos S, Massa CM, Aston-Mourney K, Funkat A, Fam BC, Hull RL, et al.

bioRxiv preprint doi: https://doi.org/10.1101/2019.12.20.884197; this version posted December 20, 2019. The copyright holder for this preprint (which was not certified by peer review) is the author/funder, who has granted bioRxiv a license to display the preprint in perpetuity. It is made available under aCC-BY 4.0 International license.

570 Differential effect of inbred mouse strain (C57BL/6, DBA/2, 129T2) on insulin secretory
571 function in response to a high fat diet. J Endocrinol. 2005;187: 45–53.
572 doi:10.1677/joe.1.06333
573 76. Cheverud JM, Lawson HA, Fawcett GL, Wang B, Pletscher LS, R. Fox A, et al. Diet-
574 dependent genetic and genomic imprinting effects on obesity in mice. Obesity. 2011;19:
575 160–170. doi:10.1038/oby.2010.141
576 77. Lawson HA, Cady JE, Partridge C, Wolf JB, Semenkovich CF, Cheverud JM. Genetic
577 effects at pleiotropic loci are context-dependent with consequences for the maintenance of
578 genetic variation in populations. PLoS Genet. 2011;7. doi:10.1371/journal.pgen.1002256
579 78. Jenkinson CP, Coletta DK, Mandarino LJ, Kashyap SR, Cornell JE, Folli F, et al. Effect of
580 acute physiological hyperinsulinemia on gene expression in human skeletal muscle in vivo.
581 Am J Physiol Metab. 2008;294: E910–E917. doi:10.1152/ajpendo.00607.2007
582 79. Gao M, Ma Y, Liu D. High-fat diet-induced adiposity, adipose inflammation, hepatic
583 steatosis and hyperinsulinemia in outbred CD-1 mice. PLoS One. 2015;10: 1–15.
584 doi:10.1371/journal.pone.0119784
585 80. Ukropec J, Koška J, Vlček M, Eckel J, Penesová A, Sell H, et al. Protein Array Reveals
586 Differentially Expressed Proteins in Subcutaneous Adipose Tissue in Obesity**. Obesity.
587 2008;15: 2396–2406. doi:10.1038/oby.2007.285
588 81. Park H, Funai K, Lodhi IJ. Peroxisome-derived lipids regulate adipose thermogenesis by
589 mediating cold-induced mitochondrial fission Find the latest version : 2018.
590 doi:10.1172/JCI120606
591 82. Carson C, Miranda MA, Macias-Velasco JF, Gunawardana S, Hughes J, Oyama S, et al.
592 Natural brown adipose expansion and remission of hyperglycemia in obese SM/J mice.
593 bioRxiv. 2019; 724369. doi:10.1101/724369
594 83. Cheverud JM, Vaughn TT, Pletscher LS, Peripato AC, Adams ES, Erikson CF, et al.
595 Genetic architecture of adiposity in the cross of LG/J and SM/J inbred mice. Mamm

bioRxiv preprint doi: https://doi.org/10.1101/2019.12.20.884197; this version posted December 20, 2019. The copyright holder for this preprint (which was not certified by peer review) is the author/funder, who has granted bioRxiv a license to display the preprint in perpetuity. It is made available under aCC-BY 4.0 International license.

596 Genome. 2001;12: 3–12. doi:10.1007/s003350010218

597 84. Miki T, Minami K, Zhang L, Morita M, Gonoi T, Shiuchi T, et al. ATP-sensitive potassium
598 channels participate in glucose uptake in skeletal muscle and adipose tissue. Am J Physiol
599 - Endocrinol Metab. 2002;283: 1178–1184. doi:10.1152/ajpendo.00313.2002

600 85. Pisani DF, Beranger GE, Corinus A, Giroud M, Ghandour RA, Altirriba J, et al. The K+
601 channel TASK1 modulates b-adrenergic response in brown adipose tissue through the
602 mineralocorticoid receptor pathway. FASEB J. 2016;30: 909–922. doi:10.1096/fj.15-
603 277475

604 86. Kuri-Harcuch W. Differentiation of 3T3-F442A Cells into Adipocytes is Inhibited by Retinoic
605 Acid. Differentiation. 1982;23: 164–169. doi:10.1111/j.1432-0436.1982.tb01279.x

606 87. Safonova I, Darimont C, Amri EZ, Grimaldi P, Ailhaud G, Reichert U, et al. Retinoids are
607 positive effectors of adipose cell differentiation. Mol Cell Endocrinol. 1994;104: 201–211.
608 doi:10.1016/0303-7207(94)90123-6

609 88. Takeda K, Sriram S, Chan XHD, Ong WK, Yeo CR, Tan B, et al. Retinoic acid mediates
610 visceral-specific adipogenic defects of human adipose-derived stem cells. Diabetes.
611 2016;65: 1164–1178. doi:10.2337/db15-1315

612 89. Frantz C, Stewart KM, Weaver VM. The extracellular matrix at a glance. J Cell Sci.
613 2010;123: 4195–4200. doi:10.1242/jcs.023820

614 90. Khan T, Muise ES, Iyengar P, Wang Z V, Chandalia M, Abate N, et al. Metabolic
615 Dysregulation and Adipose Tissue Fibrosis: Role of Collagen VI. Mol Cell Biol. 2009;29:
616 1575–1591. doi:10.1128/MCB.01300-08

617 91. Gallego R, Vázquez MJ, Martins L, Dale M, Vidal-Puig A, Hondares E, et al. BMP8B
618 Increases Brown Adipose Tissue Thermogenesis through Both Central and Peripheral
619 Actions. Cell. 2012;149: 871–885. doi:10.1016/j.cell.2012.02.066

620 92. Pellegrinelli V, Peirce VJ, Howard L, Virtue S, Türei D, Senzacqua M, et al. Adipocyte-
621 secreted BMP8b mediates adrenergic-induced remodeling of the neuro-vascular network

bioRxiv preprint doi: https://doi.org/10.1101/2019.12.20.884197; this version posted December 20, 2019. The copyright holder for this preprint (which was not certified by peer review) is the author/funder, who has granted bioRxiv a license to display the preprint in perpetuity. It is made available under aCC-BY 4.0 International license.

in adipose tissue. Nat Commun. 2018; 1–18. doi:10.1038/s41467-018-07453-x

93. Dobin A, Davis CA, Schlesinger F, Drenkow J, Zaleski C, Jha S, et al. STAR: ultrafast universal RNA-seq aligner. Bioinformatics. 2013;29: 15–21. doi:10.1093/bioinformatics/bts635

94. Kogelman LJA, Cirera S, Zhernakova D V., Fredholm M, Franke L, Kadarmideen HN. Identification of co-expression gene networks, regulatory genes and pathways for obesity based on adipose tissue RNA Sequencing in a porcine model. BMC Med Genomics. 2014;7: 1–16. doi:10.1186/1755-8794-7-57

95. Fuller TF, Ghazalpour A, Aten JE, Drake TA, Lusis AJ, Horvath S. Weighted gene coexpression network analysis strategies applied to mouse weight. Mamm Genome. 2007;18: 463–472. doi:10.1007/s00335-007-9043-3

Table 1. Differentially connected genes falling in metabolic QTL

Gene	***Col28a1***	***Kcnj14***	***Cyp26b1***	***Bmp8b***
Coordinates*	Chr6:7997808-8192617	Chr7:45816460-45824782	Chr6:84571944-84593908	Chr4:123105351-123124537
Upstream# Variants	2	0	0	0
Gene Body Variants	982	0	4	6
Downstream# Variants	8	0	0	2
QTL (Trait)	*Dserum6a* (Triglycerides)	*Ddiab7b* (AUC 10wks)	*Ddiab6c* (AUC 20wks)	*Ddiab4b* (AUC 20wks)
Module& (Traits)	brown (Glucose, GTT AUC, ITT AUC, Insulin, BAT:Body Weight)	blue (Glucose, GTT AUC, ITT AUC, BAT:Body Weight)	blue (Glucose, GTT AUC, ITT AUC, BAT:Body Weight)	red (Cholesterol, Body Weight)

* GRC38.72-mm10

1kb up- and downstream from start/stop

& brown = Cell Division; blue = Immune/Cytokine response; red = Organic metabolic processes

GTT = glucose tolerance test; ITT = insulin tolerance test; AUC = Area Under the Curve

bioRxiv preprint doi: https://doi.org/10.1101/2019.12.20.884197; this version posted December 20, 2019. The copyright holder for this preprint (which was not certified by peer review) is the author/funder, who has granted bioRxiv a license to display the preprint in perpetuity. It is made available under aCC-BY 4.0 International license.

649 **Figure Legends:**

650 **Figure 1: Brown adipose gene expression clustering by strain and diet.**

651 Dendrogram of samples clustering based on brown adipose transcriptome (top). All diet by strain
652 cohorts consist of 16 samples (8 male and 8 female) except the low fat LG cohort (8 male and 6
653 female). Phenotypic values for each sample: red = high value, white = low value, and grey =
654 missing value (bottom). Means for each cohort listed in **Supplemental Table 1**.

655

656 **Figure 2: Gene network modules correlate with variation in metabolic traits.**

657 Correlation of gene module eigenvalues with metabolic trait values. Enriched GO Terms included
658 in module name. Boxes labeled “NS” showed no significant correlation, while those labeled “LC”
659 had a significant correlation but the strength was between -0.5 and 0.5. Boxes are color coded
660 with strength of the correlation: red = high positive correlation, white = no correlation, blue = high
661 negative correlation.

662

663 **Figure 3: Principal component analysis of each individual module shows variation in diet**
664 **and strain interactions.**

665 Principal component analysis of normalized gene expression counts for each module. (**A**)
666 Variation in the immune/cytokine response module is driven mainly by strain, which further
667 separates into diet. (**B)** High fat-fed SM/J mice stand out in the cell division module. (**C** and **D)**
668 Moderate clustering in the peroxisome and organic molecule processes modules. Samples are
669 color-coded based on strain (LG/J = blue, SM/J = red) and diet (low fat = light, high fat = dark).
670 Plots are labeled with module color and enriched biological process.

671

672 **Figure 4: Genes that are both differentially expressed and differentially connected are**
673 **generally concordant in the direction of difference.**

bioRxiv preprint doi: https://doi.org/10.1101/2019.12.20.884197; this version posted December 20, 2019. The copyright holder for this preprint (which was not certified by peer review) is the author/funder, who has granted bioRxiv a license to display the preprint in perpetuity. It is made available under aCC-BY 4.0 International license.

Differential expression is plotted along the y-axis as log2 foldchange between (**A**) diets or (**B**) strains (red color indicates FDR-corrected p-value < 0.05). Connectivity is plotted along the x-axis as kdiff between (**A**) diets or (**B**) strains. Genes with a difference in connectivity above 0.5 or below -0.5 were considered differentially connected, and vertical grey dashed lines are provided to visualize these cut-offs. Horizontal grey dashed lines are also provided to visualize log2 foldchange values above 1 and below -1. Positive values indicate higher expression or connectivity in high fat-fed or SM/J cohorts, negative values indicate higher expression or connectivity in low fat-fed or LG/J cohorts.

List of Supplementary Materials:

Supplementary Figure 1: Gene network modules correlated with one or more phenotypic trait in individual diet and strain cohorts.

Supplementary Figure 2: Principal component analysis of each individual module shows variation in diet and strain interactions.

Supplementary Figure 3: Genes that are both differentially expressed and differentially connected are generally concordant in the direction of difference.

Supplementary Figure 4: Expression by cohort for four candidate genes

Supplementary Table 1: Phenotype summary statistics for each diet-by-strain cohort.

Supplementary Table 2: GO term enrichment results for all 8 brown adipose gene network modules.

Supplementary Table 3: GO term enrichment results for brown adipose gene network modules in individual diet and strain cohorts.

Supplementary Table 4: Differentially expressed and connected genes.

bioRxiv preprint doi: https://doi.org/10.1101/2019.12.20.884197; this version posted December 20, 2019. The copyright holder for this preprint (which was not certified by peer review) is the author/funder, who has granted bioRxiv a license to display the preprint in perpetuity. It is made available under aCC-BY 4.0 International license.

699 **Supplementary Table 5:** Differentially expressed and connected genes with absolute log fold

700 change ≥1 in both diet and strain comparisons.

701 **Supplementary Table 6:** List of variants between LG/J and SM/J mice in 24 hub genes.

702

703 **RNA sequencing count data available for download at:** http://lawsonlab.wustl.edu/data/

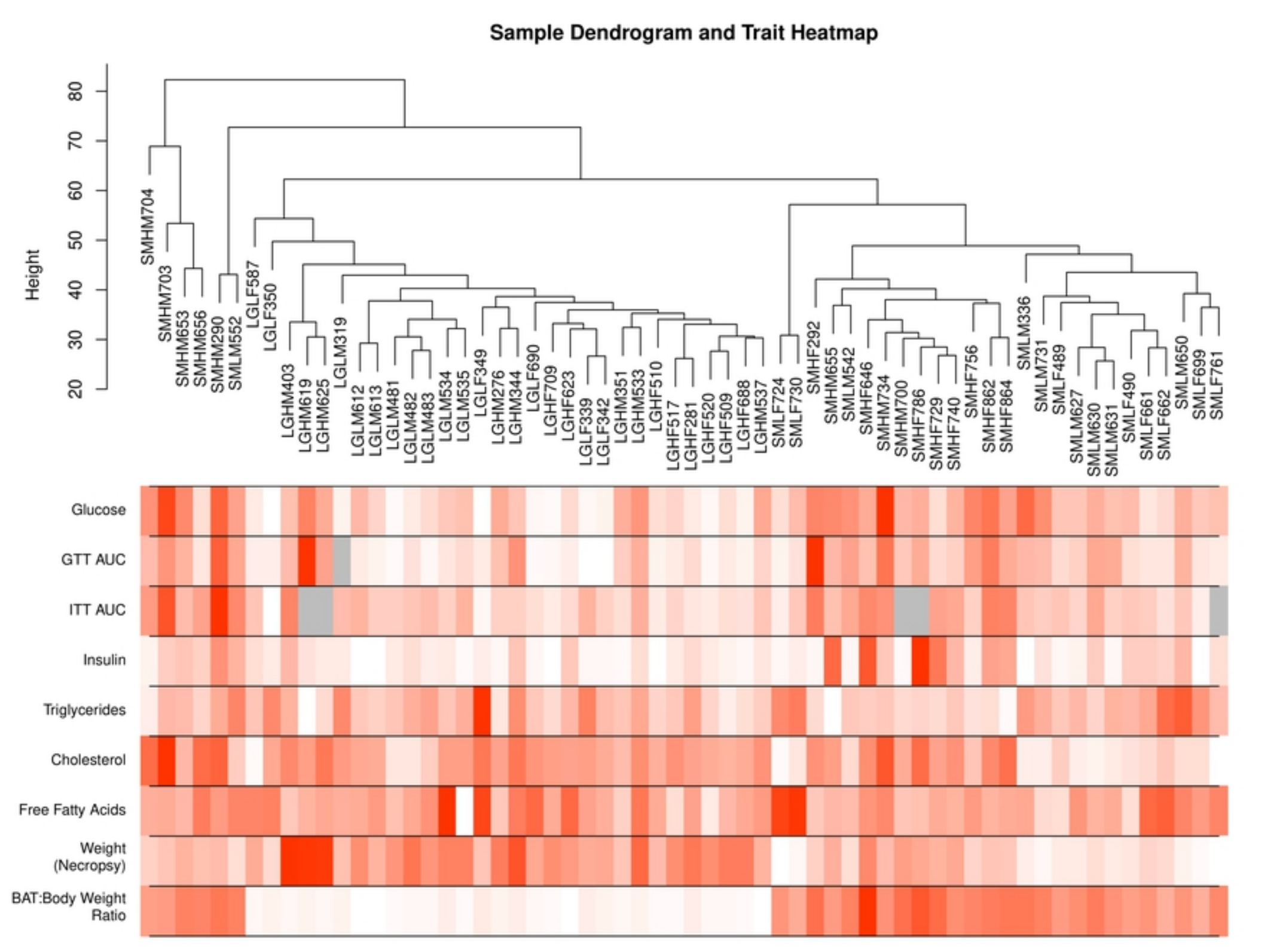
Sample Dendrogram and Trait Heatmap
Height
20
30
40
50
60
70
80
SMHM704
SMHM703
SMHM653
SMHM656
SMHM290
SMLM552
LGLF587
LGLF350
LGHM403
LGHM619
LGHM625
LGLM319
LGLM612
LGLM613
LGLM481
LGLM482
LGLM483
LGLM534
LGLM535
LGLF349
LGHM276
LGHM344
LGLF690
LGHF709
LGHF623
LGLF339
LGLF342
LGHM351
LGHM533
LGHF510
LGHF517
LGHF281
LGHF520
LGHF509
LGHF688
LGHM537
SMLF724
SMLF730
SMHF292
SMHM655
SMLM542
SMHF646
SMHM734
SMHM700
SMHF786
SMHF729
SMHF740
SMHF756
SMHF862
SMHF864
SMLM336
SMLM731
SMLF489
SMLM627
SMLM630
SMLM631
SMLF490
SMLF661
SMLF662
SMLM650
SMLF699
SMLF761
Glucose
GTT AUC
ITT AUC
Insulin
Triglycerides
Cholesterol
Free Fatty Acids
Weight (Necropsy)
BAT:Body Weight Ratio

Figure 1

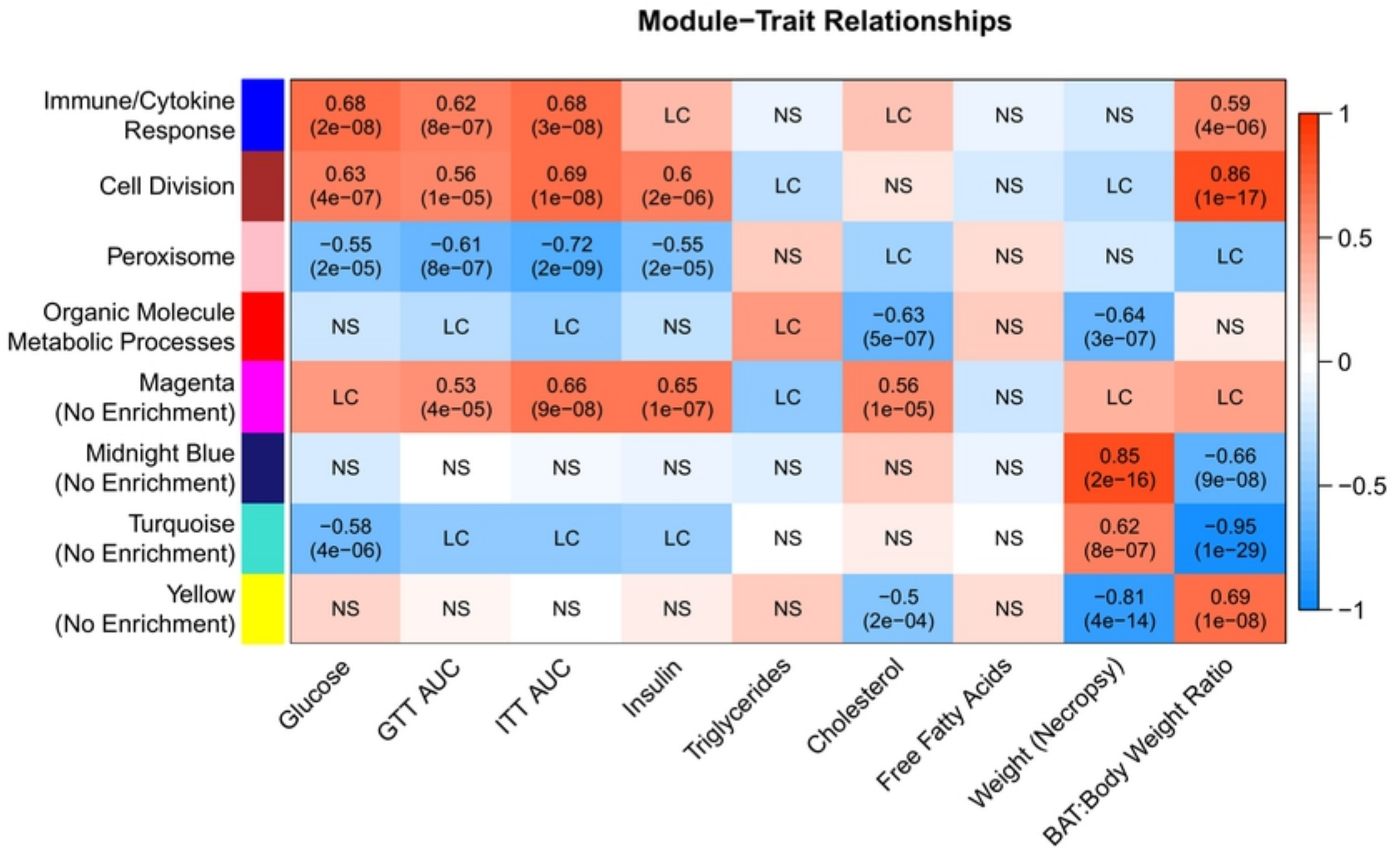
Module−Trait Relationships
Immune/Cytokine Response
Cell Division
Peroxisome
Organic Molecule Metabolic Processes
Magenta (No Enrichment)
Midnight Blue (No Enrichment)
Turquoise (No Enrichment)
Yellow (No Enrichment)
0.68 (2e−08)
0.62 (8e−07)
0.68 (3e−08)
LC
NS
LC
NS
NS
0.59 (4e−06)
0.63 (4e−07)
0.56 (1e−05)
0.69 (1e−08)
0.6 (2e−06)
LC
NS
NS
LC
0.86 (1e−17)
−0.55 (2e−05)
−0.61 (8e−07)
−0.72 (2e−09)
−0.55 (2e−05)
NS
LC
NS
NS
LC
NS
LC
LC
NS
LC
−0.63 (5e−07)
NS
−0.64 (3e−07)
NS
LC
0.53 (4e−05)
0.66 (9e−08)
0.65 (1e−07)
LC
0.56 (1e−05)
NS
LC
LC
NS
NS
NS
NS
NS
NS
0.85 (2e−16)
−0.66 (9e−08)
−0.58 (4e−06)
LC
LC
LC
NS
NS
NS
0.62 (8e−07)
−0.95 (1e−29)
NS
NS
NS
NS
NS
−0.5 (2e−04)
NS
−0.81 (4e−14)
0.69 (1e−08)
1
0.5
0
−0.5
−1
Glucose
GTT AUC
ITT AUC
Insulin
Triglycerides
Cholesterol
Free Fatty Acids
Weight (Necropsy)
BAT:Body Weight Ratio

Figure 2

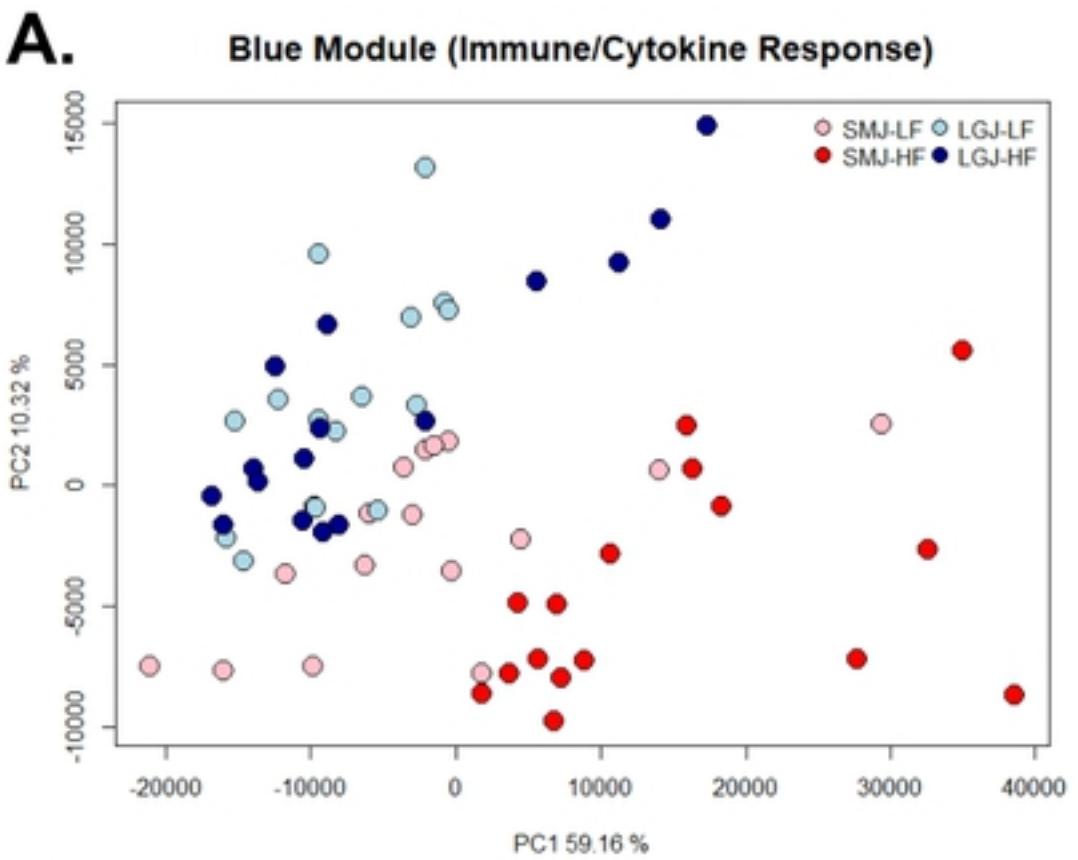
A.
Blue Module (Immune/Cytokine Response)
SMJ-LF
LGJ-LF
SMJ-HF
LGJ-HF
PC2 10.32 %
PC1 59.16 %
-20000
-10000
0
10000
20000
30000
40000
15000
10000
5000
0
-5000
-10000

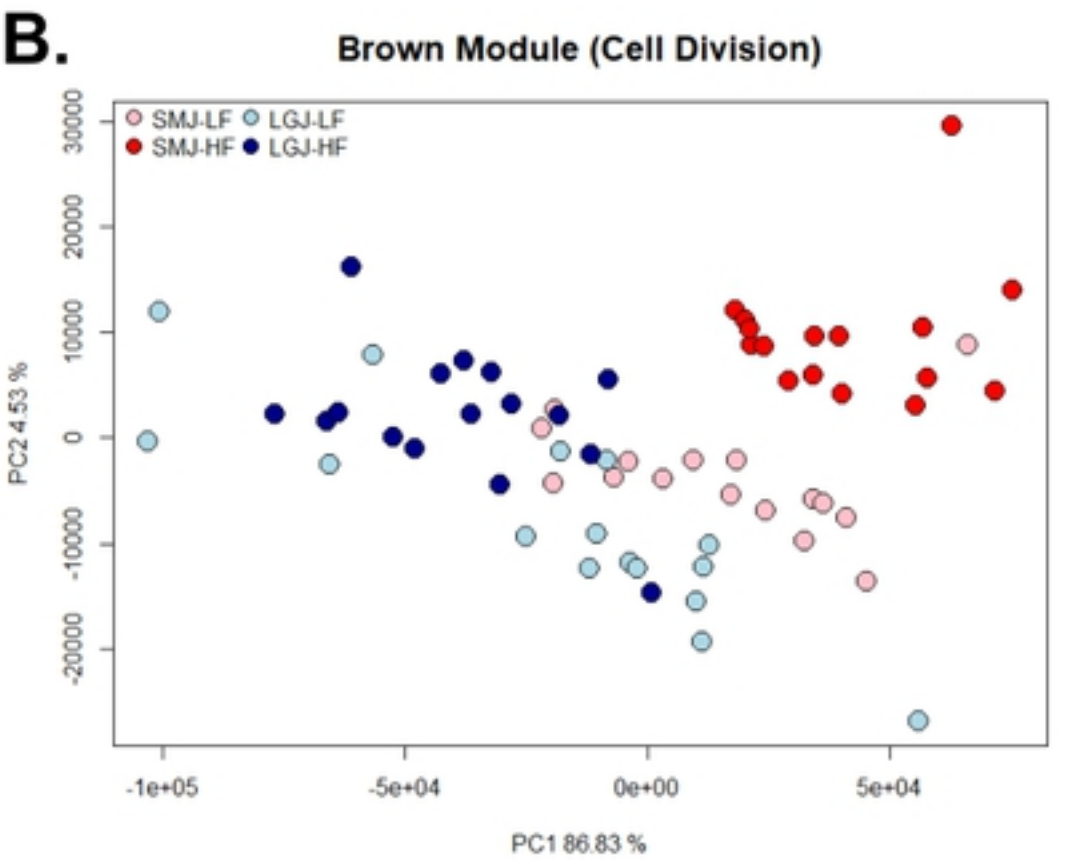
B.
Brown Module (Cell Division)
SMJ-LF
LGJ-LF
SMJ-HF
LGJ-HF
PC2 4.53 %
PC1 86.83 %
-1e+05
-5e+04
0e+00
5e+04
30000
20000
10000
0
-10000
-20000

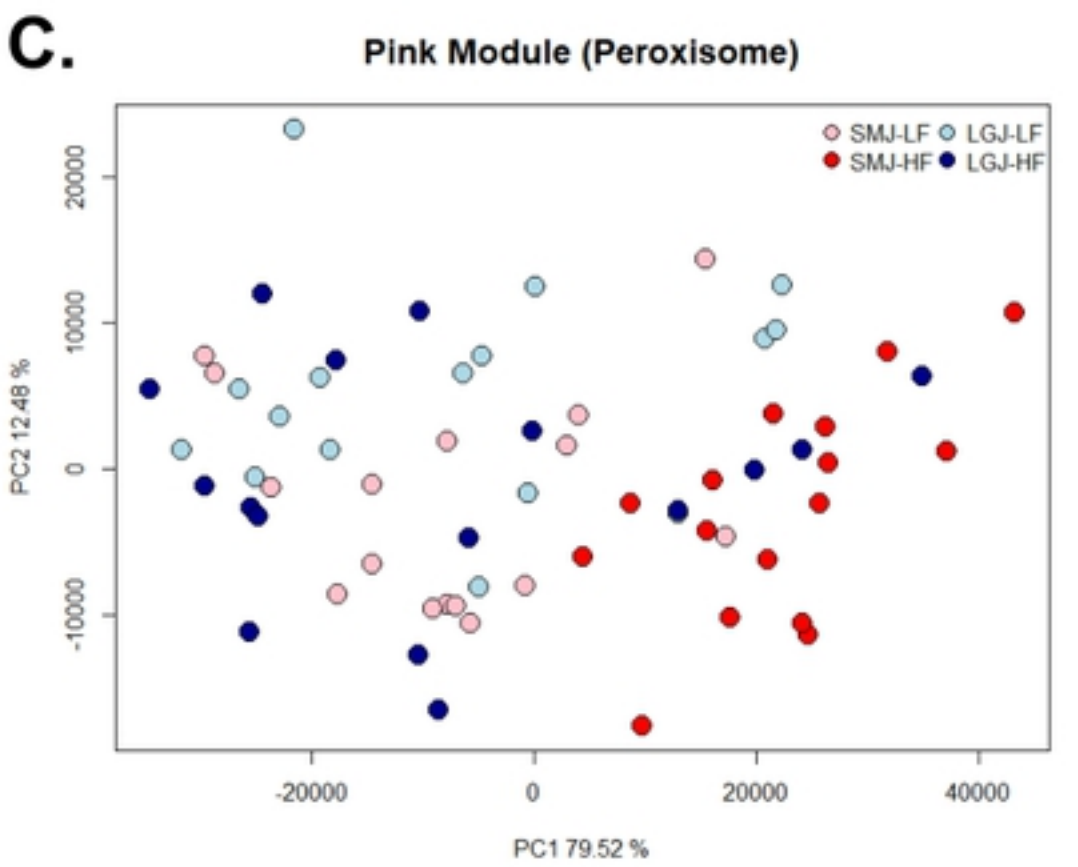
C.
Pink Module (Peroxisome)
SMJ-LF
LGJ-LF
SMJ-HF
LGJ-HF
PC2 12.48 %
PC1 79.52 %
-20000
0
20000
40000
20000
10000
0
-10000

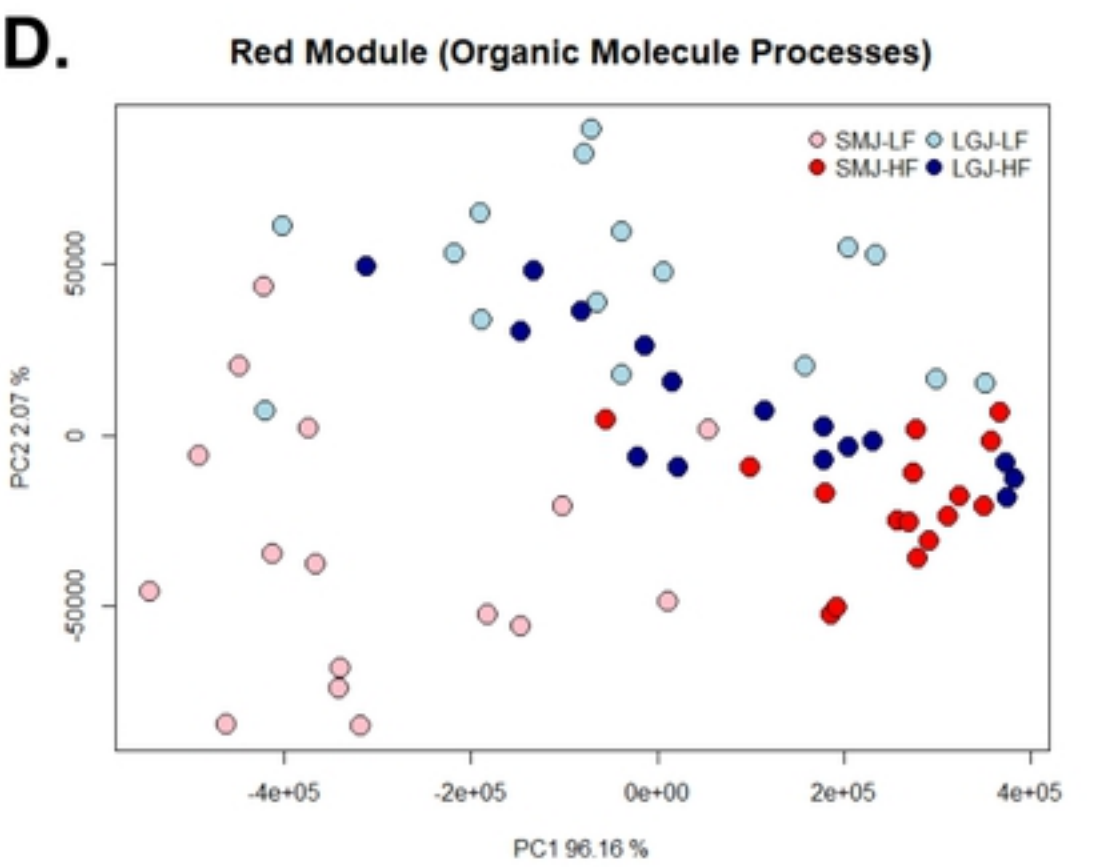
D.
Red Module (Organic Molecule Processes)
SMJ-LF
LGJ-LF
SMJ-HF
LGJ-HF
PC2 2.07 %
PC1 96.16 %
-4e+05
-2e+05
0e+00
2e+05
4e+05
50000
0
-50000

Figure 3

bioRxiv preprint doi: https://doi.org/10.1101/2019.12.20.884197; this version posted December 20, 2019. The copyright holder for this preprint (which was not certified by peer review) is the author/funder, who has granted bioRxiv a license to display the preprint in perpetuity. It is made available under aCC-BY 4.0 International license.

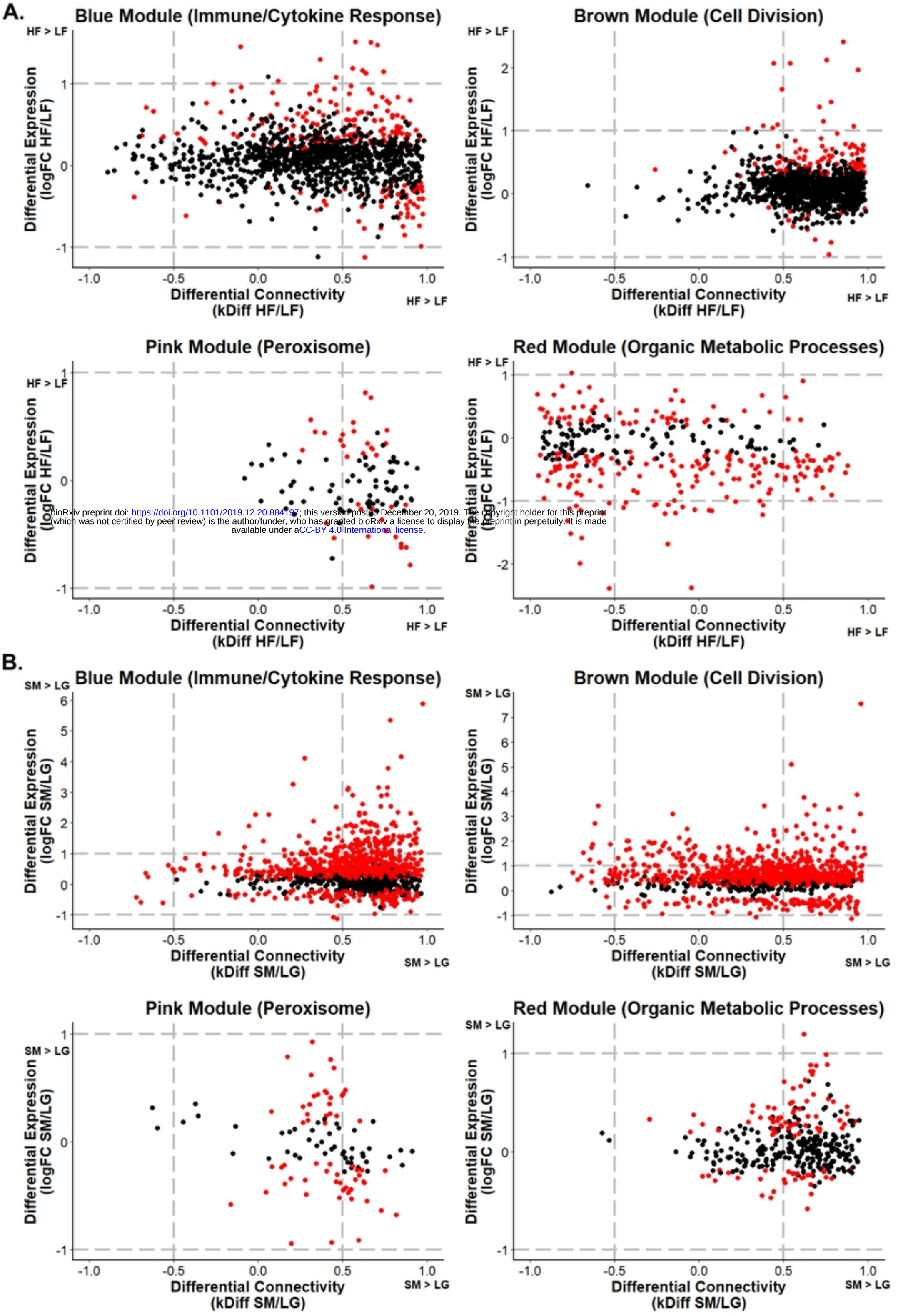

Figure 4